THE JOURNAL OF PHYSICAL CHEMISTRY C

Article

pubs.acs.org/JPCC

Laser Desorption Mass Spectrometry of End Group-Protected Linear Polyynes: Evidence of Laser-Induced Cross-Linking

Rolf W. Kirschbaum,[†] Dominik Prenzel,[‡] Stephanie Frankenberger,[‡] Rik R. Tykwinski,*[,‡] and Thomas Drewello*[,†]

[†]Physical Chemistry I, Department of Chemistry and Pharmacy, Friedrich-Alexander-University Erlangen-Nürnberg (FAU), Egerlandstrasse 3, 91058 Erlangen, Germany

[‡]Organic Chemistry I, Department of Chemistry and Pharmacy & Interdisciplinary Center for Molecular Materials (ICMM), Friedrich-Alexander-University Erlangen-Nürnberg (FAU), Henkestrasse 42, 91054 Erlangen, Germany

Supporting Information

ABSTRACT: End group-protected linear polyynes of composition Tr*−(C≡C)$_n$−Tr* (with Tr* representing the super trityl group and n = 2, 4, 6, 8, 10) and *t*Bu−(C≡C)$_6$−*t*Bu (with *t*Bu being the tertiary butyl group) have been studied by laser desorption ionization (LDI) time-of-flight (ToF) mass spectrometry. *t*Bu-terminated polyyne molecules show considerably higher stability during laser activation than Tr*-end-capped polyyne molecules. A key feature is the abundant formation of oligomeric species upon laser activation. Tandem mass spectrometry reveals strong bonding within the oligomers which indicates cross-linking of the former polyynes within the oligomers. The process is more abundantly occurring and less energy demanding than the laser-induced coalescence of C_{60}. Cross-linking is more efficient with the smaller end group (*t*Bu), and larger oligomers are formed when the chain length of the polyyne increases, both a result of enhanced interaction of the triple bonds in neighboring chains. The presence of the matrix molecules in matrix-assisted (MA)LDI hinders the polyyne interaction, and oligomer formation is markedly reduced.

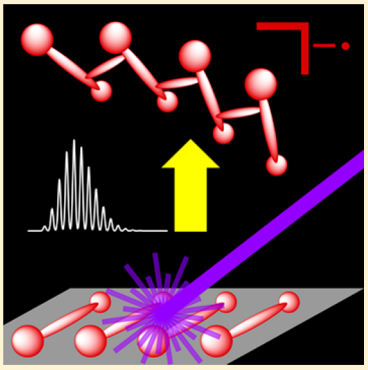

INTRODUCTION

End group-protected polyynes[1−5] can be regarded as models for carbyne, the carbon allotrope composed of sp-hybridized carbon atoms. Carbyne is the least well known of the carbon allotropes. While proposed to exist for instance in interstellar dust[6] or meteorites,[7] a sample of carbyne made in the laboratory is still pending. One major obstacle on the way from polyynes to carbyne has to be seen in the fact that the carbon chain of alternating single and triple bonds cannot be extended endlessly. In fact, after a relatively moderate number of acetylene moieties, the triple bonds of adjacent chains react with each other. This intermolecular reaction leads to cross-linking, and it is very exothermic which makes the polyynes potential explosives.[4,8] Different strategies have been developed to protect the carbon chains by sterically hindering intermolecular interactions, allowing synthetic extension of the chain length. Such approaches involved the use of bulky end groups,[9−17] sp^3 methylene chains surrounding the polyyne chain,[18−20] and rotaxanes[21−23] with end-capped polyynes threaded through a macrocycle, insulating adjacent polyynes. Proposed applications of polyyne materials are concerned with molecular electronics.[24−27]

In the present investigation, end group-protected polyynes are studied by laser desorption ionization (LDI) mass spectrometry. The experiment employs laser light for the activation of a solid sample in vacuum in combination with time-of-flight mass spectrometry for the detection of resulting ions. The polyynes under investigation are displayed in Figure 1. The title compounds are comprised of a series of polyynes of the form Tr*−(C≡C)$_n$−Tr*,[15] featuring different chain lengths with n = 2, 4, 6, 8, 10, and the "super trityl" end group (Tr* = tris(3,5-di-*tert*-butylphenyl)methyl moiety) and *t*Bu−(C≡C)$_6$−*t*Bu,[28] a hexayne terminated with the smaller *tert*-butyl end group, to allow direct comparison with Tr*−(C≡C)$_6$−Tr*.

LDI experiments with carbon allotropes are often performed with the aim to produce C_{60}. The present LDI experiment is conducted with a nitrogen laser and without a dedicated cooling or expansion device which would support the cluster formation and which is common, for instance, for the production of metal cluster ions[29,30] and, in fact, was also used in the historic formation of C_{60} from graphite by laser vaporization.[31] The C_{60} formation from graphite is rather minute with the present setup. However, C_{60} can be formed in the present experiment from a precursor whose structure is exceptionally suited for this. Related experiments include the formation of $C_{59}N$ from ligated C_{60}[32] and the conversion of a $C_{60}H_{30}$ polycyclic aromatic hydrocarbon into the C_{60} fullerene,[33] which led to its first rational synthesis.[34] LDI of a partially fluorinated precursor showed even more efficient

Received: November 10, 2014
Revised: January 10, 2015
Published: January 12, 2015

DOI: 10.1021/jp5112444
J. Phys. Chem. C 2015, 119, 2861−2870

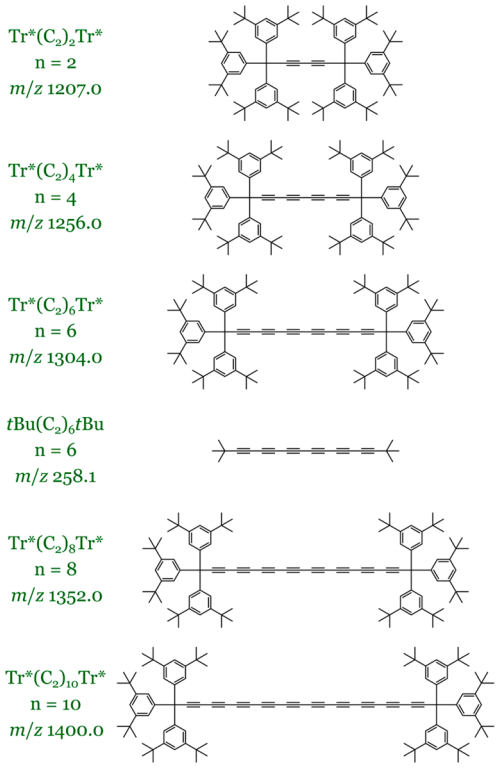

Figure 1. End group-protected polyynes under investigation: Tr*−$(C\equiv C)_n$−Tr* (Tr* = tris(3,5-di-*tert*-butylphenyl)methyl ("super trityl") group, n = 2, 4, 6, 8, and 10) and *t*Bu−$(C\equiv C)_6$−*t*Bu (*t*Bu = tertiary butyl group). Given m/z values refer to the most intense peak of the isotope envelope.

conversion into the fullerene than the PAH.[35] Of particular importance to the topic of this paper are LDI experiments of polyyne-containing precursor molecules. Tobe et al.[36] and Rubin et al.[37] independently developed a strategy for the formation of fullerenes, which applies LDI for the conversion of cyclophane-implemented three-dimensional cyclic polyynes. For C_{60}, all carbon atoms are already implemented in the precursor and the protecting groups are expelled under laser activation, followed by subsequent rearrangement to the fullerene product. Tobe et al. extended this approach to the selective formation of the larger fullerene C_{78}.[38] Initially, McElvany, Diederich and co-workers reported the coalescence of cyclocarbons by LDI of monocyclic polyyne precursors, and the resulting all-carbon ions were interpreted as fullerene structures.[39]

In this context, the following study is motivated by the intention to evaluate the behavior of linear end-capped polyynes under LDI conditions regarding ion formation, stability, and reactivity. The investigation is also intended to elucidate an earlier observation of oligomeric species in laser desorption-based analysis of monomeric polyynes.[14] The investigation of linear end-capped polyynes by LDI is unprecedented. Of particular interest in this study is the formation of oligomeric species depending on the nature of the end group and the polyyne chain length. Further experiments evaluate the nature of the bonding within the oligomers.

EXPERIMENTAL SECTION

Chemicals. Methanol (MeOH, Carl Roth, Karlsruhe), *o*-dichlorobenzene (*o*DCB, Sigma-Aldrich, Steinheim), and dichloromethane (DCM, VWR, Leuven) were used as supplied. *t*Bu−$(C\equiv C)_6$−*t*Bu and Tr*−$(C\equiv C)_n$−Tr* with n = 4, 6, 8, and 10 were prepared by the procedures given by Chalifoux and Tykwinski.[15,28]

Compound Tr*−$(C\equiv C)_2$−Tr* was prepared as follows. To a solution of Tr*-acetylene (60 mg, 0.099 mmol) in dry DMF (3 mL) and THF (3 mL) was added *i*-Pr_2NH (40 mg, 56 μL, 0.40 mmol), CuI (9.4 mg, 0.050 mmol), and $Pd(OAc)_2$ (11 mg, 0.050 mmol) and the solution stirred for 24 h at rt. Et_2O (20 mL) and saturated aq. NH_4Cl (20 mL) were added, and the layers were separated. The organic phase was washed with saturated aq. NaCl (2 × 50 mL), dried ($MgSO_4$), and filtered, and the solvent was removed in vacuo. After purification by column chromatography (silica gel, hexanes/CH_2Cl_2 10:1), the product was obtained as a white solid (48 mg, 80%). Mp 243−245 °C. R_f = 0.63 (hexanes/CH_2Cl_2 10:1). IR (ATR): 3068 (w), 2955 (s), 2904 (m), 2866 (m), 2047 (vw), 1591 (m) cm^{-1}. ^1H NMR (300 MHz, $CDCl_3$): δ 7.24 (t, J = 1.7 Hz, 6H), 6.96 (d, J = 1.7 Hz, 12H), 1.20 (s, 108H). ^{13}C NMR (75 MHz, $CDCl_3$): δ 149.7, 144.7, 123.9, 119.9, 83.9, 69.1, 57.0, 34.9, 31.5. MALDI HRMS m/z calcd for $C_{90}H_{126}$ ($M^{+\bullet}$) 1206.98541, found 1206.98489; calcd for $C_{90}H_{126}Na$ ($[M + Na]^+$) 1229.97518, found 1229.97443; calcd for $C_{90}H_{126}K$ ($[M + K]^+$) 1245.94911, found 1245.94827.

Sample Preparation. *(MA)LDI.* Solutions (mass concentration 1.0 g L^{-1}) of the polyynes in *o*DCB were prepared. For LDI, 2−5 μL of this solution was pipetted directly onto the target plate surface. To accelerate the drying of the droplets, the target was placed into a vacuum desiccator (membrane pump MZ 2C, Vacuubrand, Wertheim, Germany) until the solvent was fully evaporated. The deposition/drying procedure was repeated up to five times. For the MALDI experiments matrix stock solutions of *trans*-2-[3-(4-*tert*-butylphenyl)-2-methyl-2-propenylidene]malononitrile (DCTB) in DCM were prepared (20.0 g L^{-1}). The DCTB matrix solution and the analyte solution were combined to give a molar ratio of 1000:1. The resulting solution was deposited on the target plate (2−5 μL) and allowed to air dry. In the case where the polyyne was tagged with an Ag^+ ion, a silver trifluoroacetate (AgTFA) solution (1.0 g L^{-1} in MeOH) was added before deposition and air drying (n(DCTB)/n(polyyne)/n(AgTFA) = 1000:1:3).

ESI. An AgTFA solution (3.0×10^{-4} mol L^{-1} in MeOH) was combined with the analyte solution (1.0 g L^{-1} in *o*DCB) to give a molar ratio of n(polyyne)/n(AgTFA) = 1:3. This solution was then diluted with DCM to c(polyyne) = 5.0×10^{-5} mol L^{-1}.

Instruments. *(MA)LDI-ToF.* The (MA)LDI experiments were carried out with a Reflex IV (Bruker) mass spectrometer. The instrument is equipped with a nitrogen laser (λ = 337 nm) and was operated at the following parameters: averaged single-shot spectra 200, laser pulse repetition rate 9.0 Hz, delay time 200 ns (pulsed ion extraction). According to the instrument setup, which is explained in further detail by Ómarsson et al.,[40] the following acceleration voltages were chosen: 20.00 (ion source 1), 16.60 (ion source 2 in reflectron mode), 18.50 (ion source 2 in linear mode), and 23.0 kV (linear-field reflectron).[40,41] The mass calibration was conducted with CsI clusters (generated from CsI_3).[42] A ground steel microtiter plate (MTP 384, Bruker) was used as the target. One set of negative-ion PSD experiments was conducted with the Axima Confidence mass spectrometer (Shimadzu). The instrument operates a curved-field reflectron.

ESI-Quadrupole Ion Trap (QIT). For the electrospray experiments the sample solutions were infused via a syringe

DOI: 10.1021/jp5112444
J. Phys. Chem. C 2015, 119, 2861−2870

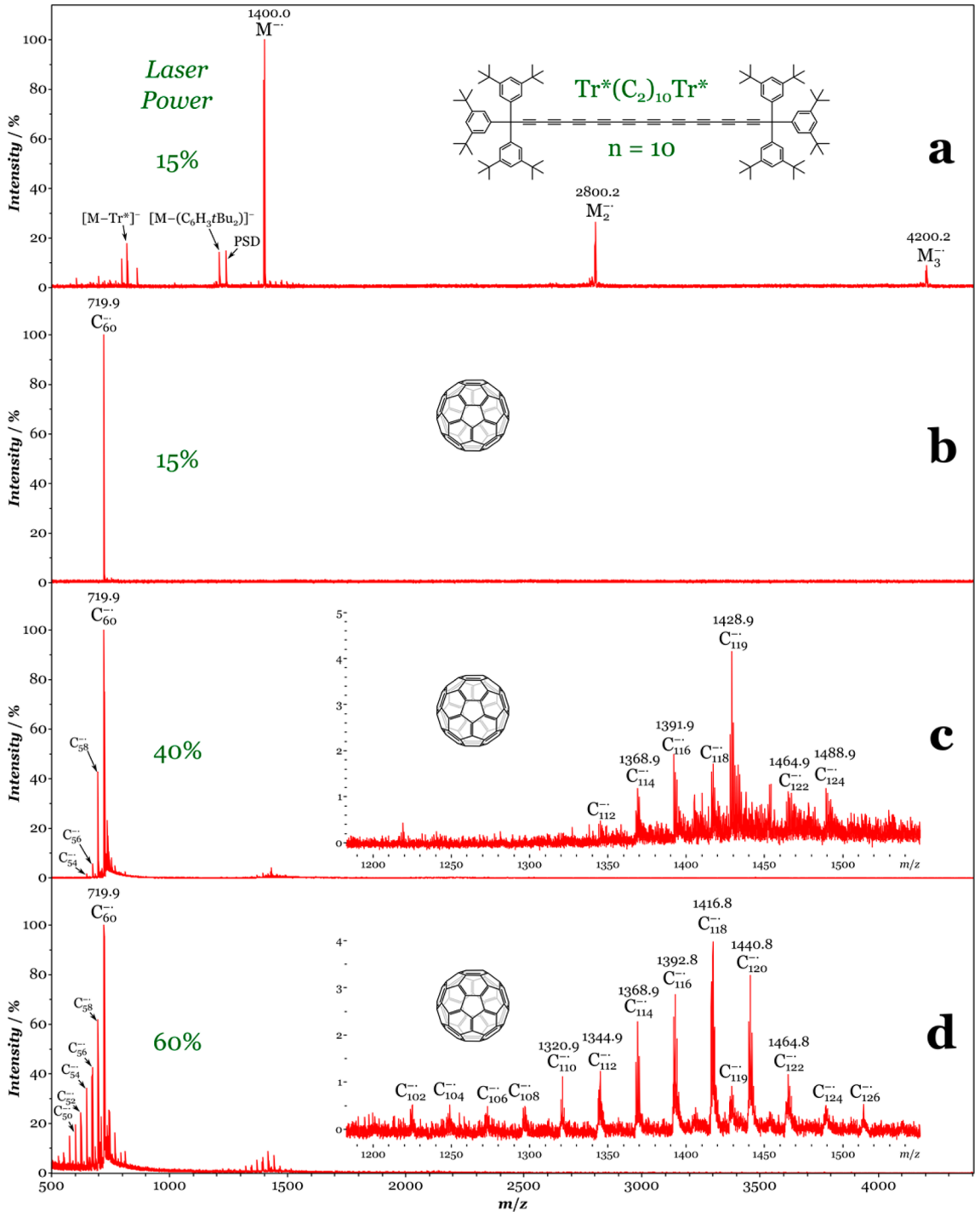

Figure 2. Comparison of polyyne oligomerization vs C_{60} coalescence. Negative-ion LDI reflectron mass spectra of (a) Tr*−(C≡C)$_{10}$−Tr* at a laser power of 15% compared to C_{60} at a laser power of (b) 15%, (c) 40%, and (d) 60%.

pump (Cole Parmer, IL) through a pneumatically assisted nebulizer (N_2) into the ESI source chamber. An esquire6000 QIT (Bruker) with the following instrumental settings was used: sample flow rate 4.0 μL/min, nebulizer nitrogen pressure 689 hPa, capillary entrance voltage −4000 kV, spray shield voltage −3500 kV, nitrogen dry gas temperature 573 K, dry gas flow rate 5.0 L/min, helium buffer/collision gas pressure was set to 4.0×10^{-6} hPa (the actual pressure in the analyzer is approximately 100 times higher[43]). Generally, the ion transfer settings vary due to spectra tuning.

RESULTS AND DISCUSSION

Figure 2a shows a partial laser desorption mass spectrum of the polyyne Tr*−(C≡C)$_{10}$−Tr* obtained in the negative-ion mode. The unusual finding is the extent by which oligomers are produced during the experiment. Other data leave no doubt that the compound is a clean monomer prior to the laser activation.[11] Evidently, LDI induces the efficient formation of oligomers, which could be detected up to the hexamer in this experiment (not shown). Both the extent of the oligomerization and the low laser fluence required to achieve cross-linking

DOI: 10.1021/jp5112444
J. Phys. Chem. C 2015, 119, 2861−2870

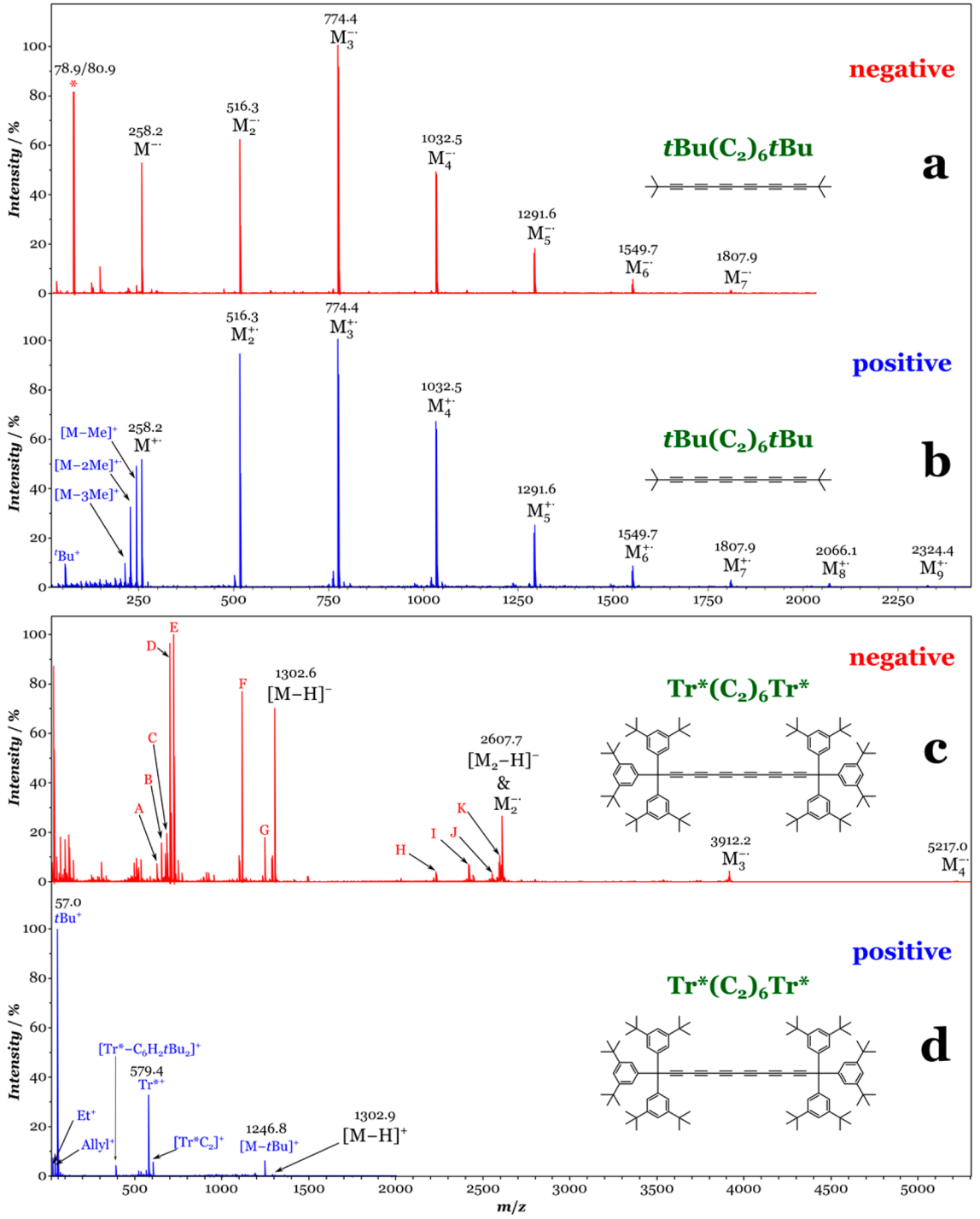

Figure 3. LDI reflectron mass spectrum of *t*Bu−(C≡C)$_6$−*t*Bu ((a) negative and (b) positive ions) and Tr*−(C≡C)$_6$−Tr* ((c) negative and (d) positive ions). Asterisk (*) = Br^- (from synthesis), A = $[M - Tr^*C_8]^-$, B = $[M - Tr^*C_6]^-$, C $[M - Tr^*C_4]^-$, D = $[M - Tr^*C_2]^-$, E = $[M - Tr^*]^-$, F = $[M - C_6H_3tBu_2]^-$, G = $[M - tBu]^-$, H = $[M_2 - 2C_6H_3tBu_2]^{-\bullet}$ and $[M_2 - H - 2C_6H_3tBu_2]^-$, I = $[M_2 - C_6H_3tBu_2]^-$, J = $[M_2 - tBu]^-$, K = $[M_2 - Me]^-$.

are remarkable. We illustrate this by comparison with the well-established coalescence reactivity of C_{60}[44] in the same experimental run. The laser fluence is given as a laser power percentage. This value relates to the actual laser fluence relative to a maximum value. For the polyyne we have been unable to obtain a mass spectrum without oligomers. Even at the lowest laser power required to observe a monomer ion this was always accompanied by a dimer and trimer ion. This indicates that the laser desorption of the material is directly connected with the oligomerization of the monomers. Polyyne oligomers are efficiently formed at 15% laser power (Figure 2a), while C_{60} (Figure 2b) only shows the $C_{60}^{-\bullet}$ radical anion without any sign of coalescence. At a laser power of 40%, the first coalescence signals are slowly emerging (Figure 2c), featuring a maximum abundance at 60% laser power. Even at this value the abundance of coalescence products remains behind the production of the oligomeric polyynes (Figure 2a). The high degree of uneven covalent carbon dimer ions is likely caused by

DOI: 10.1021/jp5112444
J. Phys. Chem. C 2015, 119, 2861−2870

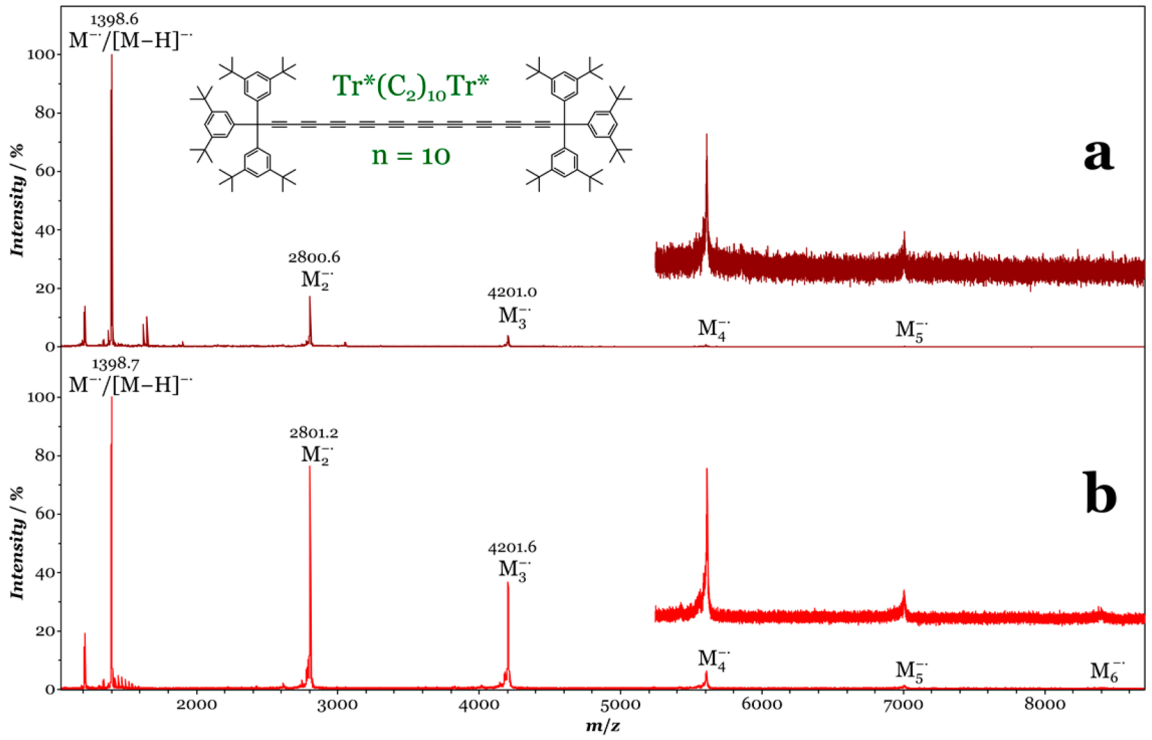

Figure 4. Mass spectrum of Tr*−(C≡C)$_{10}$−Tr* obtained by (a) MALDI (linear mode, using DCTB as matrix) and (b) direct LDI (linear mode).

CO loss occurring from a partially oxidized C_{60} sample. However, C_{60} oxides have been shown to have an even higher tendency to coalesce than C_{60} itself.[45] In summary, the polyyne oligomer formation occurs at very low laser power, literally accompanying the desorption/ionization process of the monomer. However, distinction between noncovalent clustering (e.g., by $\pi-\pi$ interactions) and covalent bonding (by chemical reactions) is not possible by analysis of the mass-to-charge ratio of the oligomers/clusters. Tandem mass spectrometry, as performed below, is required to investigate the difference in the stability of the observed oligomers/clusters.

The next set of experiments investigates the influence of the size of the end group and the polarity of the charge on the production of the oligomer ions. Figure 3 compares the LDI mass spectra of *t*Bu−(C≡C)$_6$−*t*Bu and Tr*−(C≡C)$_6$−Tr* in both ion modes. The *t*Bu−(C≡C)$_6$−*t*Bu target displays enhanced oligomerization in both ion modes. The trimer is clearly more abundant than the dimer with a generally more pronounced oligomer abundance. This clearly indicates that oligomerization is facilitated for the polyyne with the end group that is less sterically demanding. The *t*Bu−(C≡C)$_6$−*t*Bu target also reveals that oligomerization occurs quite readily in both ion modes. The Tr*−(C≡C)$_6$−Tr* molecular ion shows a strong degree of fragmentation in both ion modes. In the positive-ion mode the decomposition is so severe that the monomeric ion is hardly observed and oligomerization is prevented because of decomposition (Figure 3d). In the negative-ion mode fragmentations are also abundant, but the molecular anion of the monomeric polyyne is nonetheless abundantly observed even at the highest laser power available, and the oligomerization process can also occur (Figure 3c). The fragmentation patterns of both ion modes suggest that the decomposition is caused by the decay of the Tr* group itself and by the loss of Tr* from the chain rather than by decay of the central polyyne chain. Ironically, protection by the Tr* group allowed the synthesis of the longest polyyne to date,[15] but under the present conditions it is decomposition (in the positive-ion mode) rather than protection which prevents oligomerization.

The influence of the chain length on the oligomerization has been evaluated in LDI experiments studying separate targets of Tr*−(C≡C)$_n$−Tr* with n = 2, 4, 6, 8, and 10. Since the decomposition of the Tr*-terminated polyynes severely affects the oligomerization process in the positive-ion mode (Figure 3d), the experiments were conducted in the negative-ion mode, and the resulting spectra are shown as Figure S1, Supporting Information. The data clearly show that the oligomerization process becomes more pronounced with increasing chain length. For n = 2, the dimer ion is barely seen with the trimer ion being entirely absent. For n = 4, dimer formation is enhanced, and for n = 6 and 8, oligomers up to the tetramer can be observed with increasing abundance. Going from n = 8 to n = 10, the extent of oligomerization does not appear to be enhanced but is equally high.

MALDI is a modification of the direct LDI experiment in that a matrix material is added to the sample molecule with the intention of bringing a certain softness to the material desorption and to aid the ionization of the sample. The method has revolutionized the way large molecules are studied by mass spectrometry. While mostly applicable to large molecules of biological origin,[46] MALDI has also greatly contributed to material sciences, notably to the area of polymer analysis.[47] MALDI has been also successfully applied to the analysis of fullerene derivatives.[48−51] The matrix material DCTB has shown excellent performance in this context, with often very abundant molecular ions and avoiding unwanted fragmentation. The ionization of the analyte with DCTB works by electron transfer between DCTB ions and the sample molecule.[52,53] DCTB is also used as the matrix in the present MALDI analysis of the polyynes. A representative spectrum is

DOI: 10.1021/jp5112444
J. Phys. Chem. C 2015, 119, 2861−2870

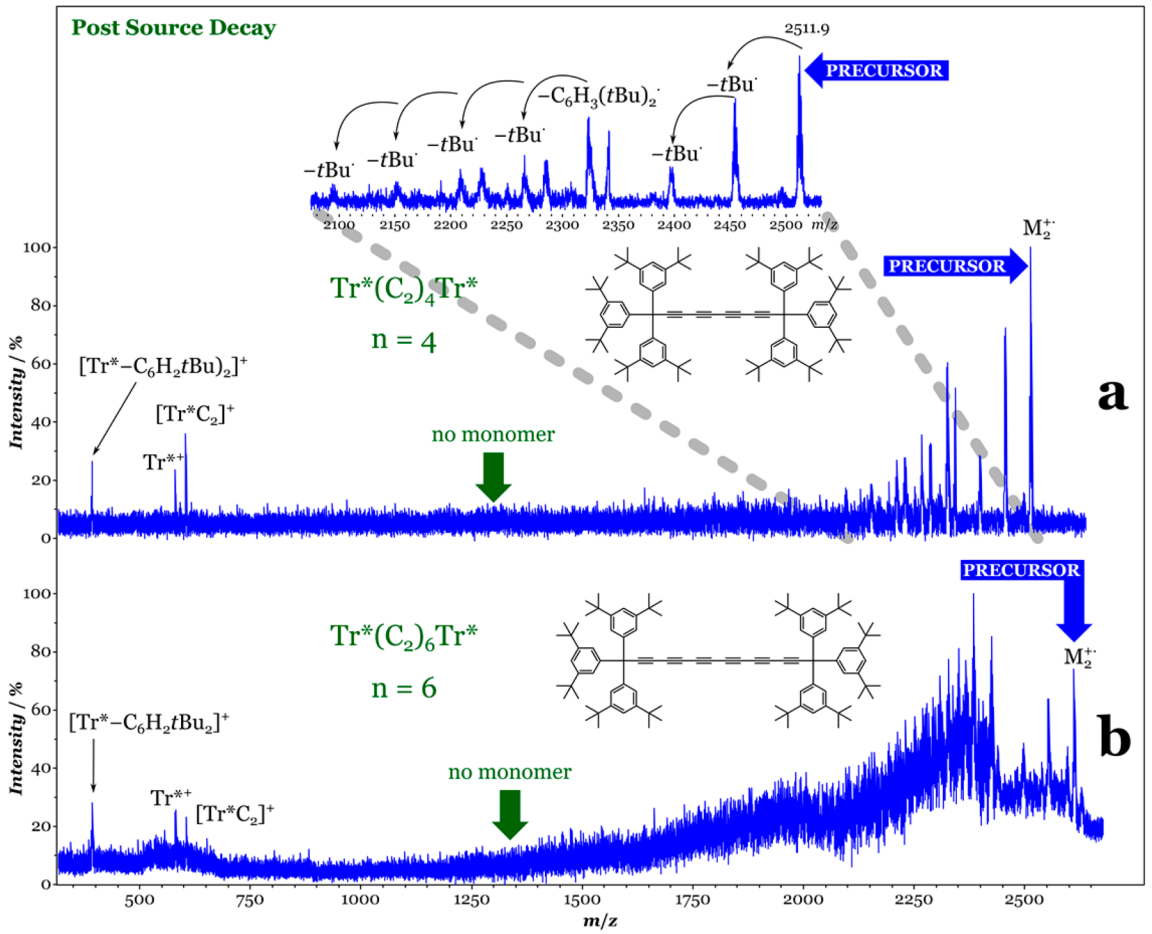

Figure 5. Positive-ion PSD mass spectrum (following LDI) of (a) the $[(Tr^*-(C{\equiv}C)_4-Tr^*)_2]^{+\bullet}$ dimer and (b) the $[(Tr^*-(C{\equiv}C)_6-Tr^*)_2]^{+\bullet}$ dimer. Positively charged oligomeric ions do not show loss of intact neutral monomer moieties, indicating strong covalent cross-linking within the oligomers. Negatively charged oligomers show a similar behavior (Figure S4, Supporting Information).

shown in Figure 4a and compared to the direct LDI experiment in Figure 4b. The most striking difference between the two approaches is the reduced presence of oligomeric ions in the MALDI experiment (Figure 4a). Evidently, the presence of the matrix hinders oligomerization, which is straightforwardly explained by the matrix blocking the interaction between the monomers. Apart from hindering oligomerization, MALDI shows less dissociations of the monomer at elevated laser powers. An overview of LDI (Figure S2, Supporting Information) and MALDI (Figure S3, Supporting Information) mass spectra at varying laser powers is shown in the Supporting Information.

The final set of experiments is devoted to the elucidation of the nature of the bonding between the monomer units within the oligomers. For this purpose, tandem mass spectrometry in the form of postsource decay (PSD) experiments was performed. In this experiment, the fragment ions of a chosen precursor ion of interest were recorded. The underlying principle of the PSD experiment has been outlined recently in the context of the ions derived from fullerene/crown ether conjugates.[54] In light of the exothermicity of polyyne/polyyne reactions, it is not very likely that the present LDI experiment would result in loosely bound oligomers. Hypothetically, a loosely bound oligomer ion in which the structural integrity of its monomeric building blocks is retained would dissociate upon activation by loss of these monomer units, reflecting the fact that bonding between monomer units is not as strong as the bonding within the monomer moiety itself. The recently discovered gas-phase aggregates of superbenzene−porphyrin conjugates, which feature only noncovalent bonding between monomers, may serve as an example of this type of ion.[55] The crystal sructures of perfluorophenyl end-capped polyynes provided by Tykwinski et al. may serve to illustrate noncovalent bonding in polyyne clusters.[14] By contrast, strong covalent bonding between the monomers can only be achieved by cross-linking through the involvement of the (former) triple bonds. Strong bonding between the monomer units will lead to structural changes, and fragmentation of the implemented monomer moiety will become energetically more feasible. PSD experiments were performed with numerous monomeric and oligomeric ions in both ion modes. Representative PSD mass spectra are shown in Figures 5 and S4, Supporting Information. Figure 5 shows the decay of $[(Tr^*-(C{\equiv}C)_n-Tr^*)_2]^{+\bullet}$ with n = 4 and 6 as an example of the positive ions, and Figure S4, Supporting Information, displays dissociations of $[(Tr^*-(C{\equiv}C)_{10}-Tr^*)_m]^{-\bullet}$ with m = 1, 2, 3 in the negative-ion mode. The PSD experiments showed a common behavior in that the monomer ion would lose certain parts of the end groups, while dimer and trimer ions would show the same losses only to a smaller extent. The essential observation, however, is that none of the oligomeric ions showed individual monomer losses, clearly indicating that strong cross-linking had occurred between the monomers upon laser activation. Occasionally a dimer ion would show minute amounts of a monomer fragment

DOI: 10.1021/jp5112444
J. Phys. Chem. C 2015, 119, 2861−2870

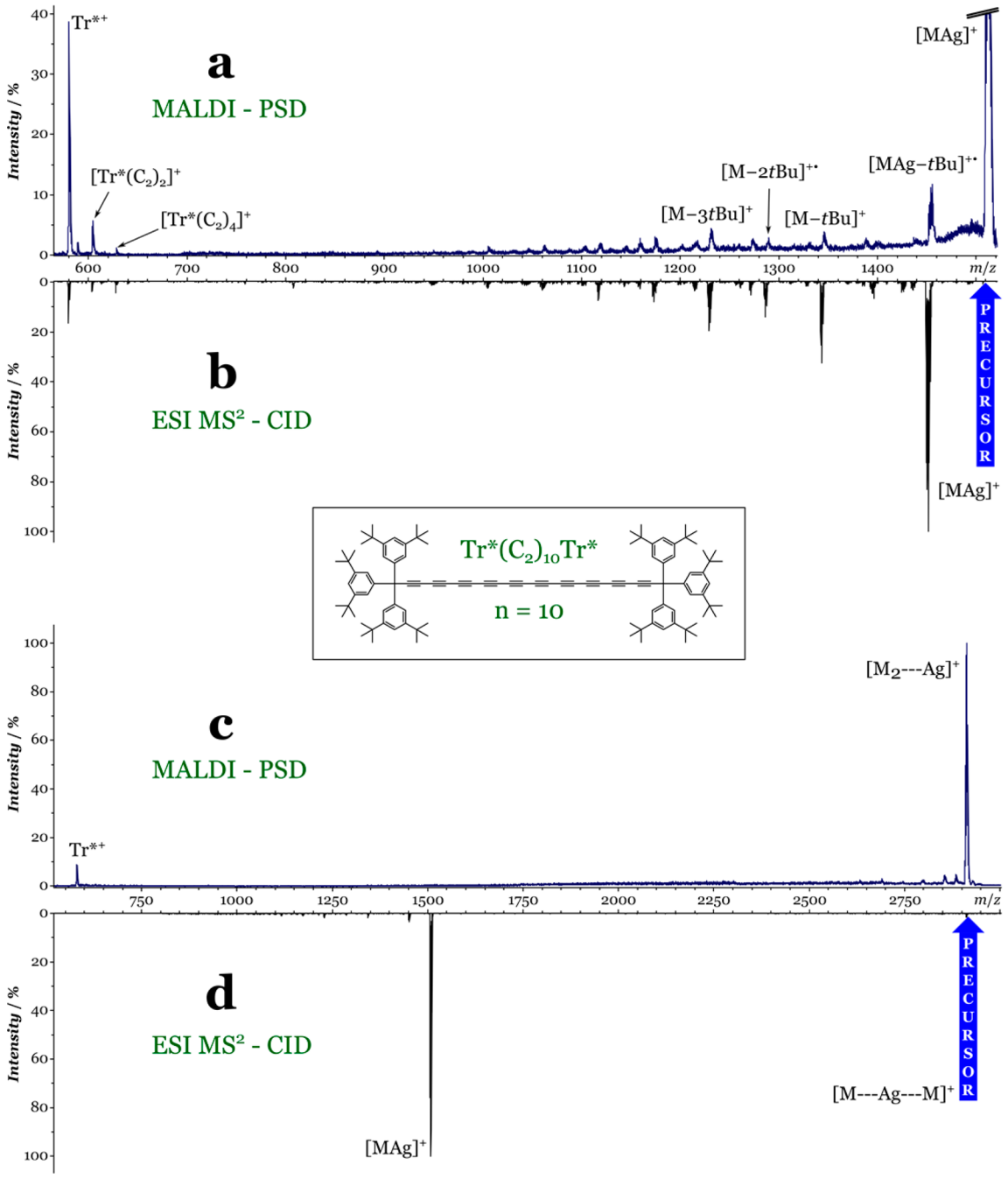

Figure 6. Comparison of the fragmentation pattern of Tr*−(C≡C)$_{10}$−Tr*/Ag$^+$ obtained by (a) PSD (following MALDI) and (b) He-CID (following ESI), (Tr*−(C≡C)$_{10}$−Tr*)$_2$/Ag$^+$ obtained by (c) PSD (following MALDI), and Tr*−(C≡C)$_{10}$−Tr*/Ag$^+$/Tr*−(C≡C)$_{10}$−Tr* obtained by (d) He-CID (following ESI). CID spectra (b and d) are displayed upside down to allow better comparison with the corresponding (upright) PSD spectra (a and c).

ion; however, the vast majority of the dimer ion population still shows strong covalent cross-linking.

The apparent lack of noncovalently bound polyyne aggregates in the LDI experiment prevents from documenting the proposed dissociation behavior of neutral monomer losses for this particular compound class. To illustrate the distinction between a strongly cross-linked oligomer and one with only loosely bound monomeric units (i.e., covalent versus noncovalent), we turned to electrospray ionization to generate a model ion of that latter category. The Ag$^+$-bound polyyne dimer (Polyyne/Ag$^+$/Polyyne) has been generated by ESI as a model ion for a noncovalently bound oligomer. The collision-induced dissociations (CID) of this ion have been compared with the PSD spectrum of an Ag$^+$-tagged cross-linked dimer generated by MALDI. First, we contrast the PSD spectrum (Figure 6a) of a monomer cationized with Ag$^+$ and generated by MALDI with the CID spectrum of the same ion generated by ESI (Figure 6b). Obviously, both dissociation approaches result in similar daughter ion spectra. Both PSD and CID provide the same daughter ion signals, only with different abundances. Thus, both are suited to dissociate the ion for structure elucidation. In Figure 6c, the PSD spectrum of the dimer generated by MALDI and cationized by attachment of Ag$^+$ is shown and contrasted with the CID spectrum of an ion

DOI: 10.1021/jp5112444
J. Phys. Chem. C 2015, 119, 2861−2870

of the same composition generated in ESI (Figure 6d). While the covalently bound dimer ions show the loss of a Tr^{*+} group as a charged fragment, the noncovalent dimer dissociates as expected by the loss of the intact monomer unit.

The present findings have to be seen in the context of light-induced polymerization of polyynes occurring in the solid state. These reactions have been known for a long time[4,56,57] and in recent years led to modern applications within the preparation of carbon nanomaterials.[58,59] In the present experiments oligomerization may occur through both photopolymerization within the target and ion/molecule reactions in the expanding material plume following laser ablation. The nature of the covalent cross-linking remains unclear in the present investigation. However, in Figure S5, Supporting Information, speculative structural motifs are given as possibly derived by photo-oligomerization and ion/molecule dimerization of polyynes. The LDI approach provides a unique tool in that products of the laser-induced oligomerization are directly sampled as individual ions following the desorption/ionization process. While the ion distribution will be clearly influenced by the efficiencies of the different processes, including fragmentation, the essential advantage, however, has to be seen in the fact that the obtained ion distribution still allows one to get insight into the importance of oligomerization as a function of structural features of the polyyne target under study, as demonstrated in this report.

CONCLUSIONS

Laser desorption of end group-protected polyynes is accompanied by oligomerization, mediated through covalent cross-linking. The process is more prevalent with smaller end groups as well as for polyynes with increasing number of acetylene moieties up to n = 8 or 10. In MALDI, the matrix molecules hinder the cross-linking process. Polyynes with Tr* (super trityl) end groups show significant fragmentation under LDI conditions. Polyynes with *t*Bu end groups are more resistant to fragmentation. The LDI experiment provides an excellent tool to evaluate the tendency toward oligomerization as a function of structural features of the polyyne.

ASSOCIATED CONTENT

Supporting Information

Negative-ion direct LDI mass spectra of Tr*−$(C{\equiv}C)_n$−Tr* with n = 2, 4, 6, 8, 10; negative-ion direct LDI mass spectra of Tr*−$(C{\equiv}C)_{10}$−Tr* at different laser power settings; negative-ion MALDI mass spectra of Tr*−$(C{\equiv}C)_{10}$−Tr* at different *laser power* settings; PSD mass spectra of the super trityl end-capped decayne mono-, di-, and trimer radical anion (following LDI); structural motifs of covalently cross-linked polyynes. This material is available free of charge via the Internet at http://pubs.acs.org.

AUTHOR INFORMATION

Corresponding Authors

*E-mail: rik.tykwinski@fau.de.
*E-mail: thomas.drewello@fau.de.

Notes

The authors declare no competing financial interest.

ACKNOWLEDGMENTS

The authors thank the Deutsche Forschungsgemeinschaft (DFG)−SFB 953 "Synthetic Carbon Allotropes" for financial support.

REFERENCES

(1) Diederich, F. Carbon Scaffolding: Building Acetylenic All-Carbon and Carbon-Rich Compounds. *Nature* **1994**, *369*, 199−207.
(2) Chalifoux, W. A.; Tykwinski, R. R. Synthesis of Extended Polyynes: Toward Carbyne. *C. R. Chim.* **2009**, *12*, 341−358.
(3) Szafert, S.; Gladysz, J. A. Update 1 of: Carbon in One Dimension: Structural Analysis of the Higher Conjugated Polyynes. *Chem. Rev.* **2006**, *106*, PR1−PR33.
(4) Chernick, E. T.; Tykwinski, R. R. Carbon-Rich Nanostructures: The Conversion of Acetylenes Into Materials. *J. Phys. Org. Chem.* **2013**, *26*, 742−749.
(5) Schermann, G.; Grösser, T.; Hampel, F.; Hirsch, A. Dicyanopolyynes: A Homologuous Series of End-Capped Linear sp Carbon. *Chem.—Eur. J.* **1997**, *3*, 1105−1112.
(6) Webster, A. Carbyne as a Possible Constituent of the Interstellar Dust. *Mon. Not. R. Astron. Soc.* **1980**, *192*, 7−9.
(7) Hayatsu, R.; Scott, R. G.; Studier, M. H.; Lewis, R. S.; Anders, E. Carbynes in Meteorites: Detection, Low-Temperature Origin, and Implications for Interstellar Molecules. *Science* **1980**, *209*, 1515−1518.
(8) Armitage, J. B.; Entwistle, N.; Jones, E. R. H.; Whiting, M. C. Researches on Acetylenic Compounds. Part XLI. The Synthesis of Diphenylpolyacetylenes. *J. Chem. Soc.* **1954**, 147−154.
(9) Johnson, T. R.; Walton, D. R. M. Silylation as a Protective Method in Acetylene Chemistry: Polyyne Chain Extensions Using the Reagents, $Et_3Si(C{\equiv}C)_mH$ (m = 1,2,4) in Mixed Oxidative Couplings. *Tetrahedron* **1972**, *28*, 5221−5236.
(10) Gibtner, T.; Hampel, F.; Gisselbrecht, J.-P.; Hirsch, A. End-Cap Stabilized Oligoynes: Model Compounds for the Linear sp Carbon Allotrope Carbyne. *Chem.—Eur. J.* **2002**, *8*, 408−432.
(11) Luu, T.; Elliott, E.; Slepkov, A. D.; Eisler, S.; McDonald, R.; Hegmann, F. A.; Tykwinski, R. R. Synthesis, Structure, and Nonlinear Optical Properties of Diarylpolyynes. *Org. Lett.* **2005**, *7*, 51−54.
(12) Eisler, S.; Slepkov, A. D.; Elliott, E.; Luu, T.; McDonald, R.; Hegmann, F. A.; Tykwinski, R. R. Polyynes as a Model for Carbyne: Synthesis, Physical Properties, and Nonlinear Optical Response. *J. Am. Chem. Soc.* **2005**, *127*, 2666−2676.
(13) Zheng, Q.; Bohling, J. C.; Peters, T. B.; Frisch, A. C.; Hampel, F.; Gladysz, J. A. A Synthetic Breakthrough Into an Unanticipated Stability Regime: A Series of Isolable Complexes in Which C_6, C_8, C_{10}, C_{12}, C_{16}, C_{20}, C_{24}, and C_{28} Polyynediyl Chains Span Two Platinum Atoms. *Chem.—Eur. J.* **2006**, *12*, 6486−6505.
(14) Kendall, J.; McDonald, R.; Ferguson, M. J.; Tykwinski, R. R. Synthesis and Solid-State Structure of Perfluorophenyl End-Capped Polyynes. *Org. Lett.* **2008**, *10*, 2163−2166.
(15) Chalifoux, W. A.; Tykwinski, R. R. Synthesis of Polyynes to Model the sp-Carbon Allotrope Carbyne. *Nat. Chem.* **2010**, *2*, 967−971.
(16) Frank, B. B.; Laporta, P. R.; Breiten, B.; Kuzyk, M. C.; Jarowski, P. D.; Schweizer, W. B.; Seiler, P.; Biaggio, I.; Boudon, C.; Gisselbrecht, J.-P.; et al. Comparison of CC Triple and Double Bonds as Spacers in Push−Pull Chromophores. *Eur. J. Org. Chem.* **2011**, *2011*, 4307−4317.
(17) Simpkins, S. M. E.; Weller, M. D.; Cox, L. R. *β*-Chlorovinylsilanes as Masked Alkynes in Oligoyne Assembly: Synthesis of the First Aryl-End-Capped Dodecayne. *Chem. Commun.* **2007**, 4035−4037.
(18) Klinger, C.; Vostrowsky, O.; Hirsch, A. Synthesis of Alkylene-Bridged Diphenyl-Oligoynes. *Eur. J. Org. Chem.* **2006**, *2006*, 1508−1524.
(19) Stahl, J.; Mohr, W.; de Quadras, L.; Peters, T. B.; Bohling, J. C.; Martín-Alvarez, J. M.; Owen, G. R.; Hampel, F.; Gladysz, J. A. sp Carbon Chains Surrounded by sp^3 Carbon Double Helices: Coordination-Driven Self-Assembly of Wirelike $Pt(C{\equiv}C)_nPt$ Moieties

DOI: 10.1021/jp5112444
J. Phys. Chem. C 2015, 119, 2861−2870

That Are Spanned by Two $P(CH_2)_mP$ Linkages. *J. Am. Chem. Soc.* **2007**, *129*, 8282−8295.
(20) de Quadras, L.; Bauer, E. B.; Mohr, W.; Bohling, J. C.; Peters, T. B.; Martín-Alvarez, J. M.; Hampel, F.; Gladysz, J. A. sp Carbon Chains Surrounded by sp^3 Carbon Double Helices: Directed Syntheses of Wirelike $Pt(C{\equiv}C)_nPt$ Moieties That Are Spanned by Two $P(CH_2)_mP$ Linkages Via Alkene Metathesis. *J. Am. Chem. Soc.* **2007**, *129*, 8296−8309.
(21) Weisbach, N.; Baranova, Z.; Gauthier, S.; Reibenspies, J. H.; Gladysz, J. A. A New Type of Insulated Molecular Wire: A Rotaxane Derived From a Metal-Capped Conjugated Tetrayne. *Chem. Commun.* **2012**, *48*, 7562−7564.
(22) Movsisyan, L. D.; Kondratuk, D. V.; Franz, M.; Thompson, A. L.; Tykwinski, R. R.; Anderson, H. L. Synthesis of Polyyne Rotaxanes. *Org. Lett.* **2012**, *14*, 3424−3426.
(23) Sahnoune, H.; Baranová, Z.; Bhuvanesh, N.; Gladysz, J. A.; Halet, J.-F. A Metal-Capped Conjugated Polyyne Threaded Through a Phenanthroline-Based Macrocycle. Probing Beyond the Mechanical Bond to Interactions in Interlocked Molecular Architectures. *Organometallics* **2013**, *32*, 6360−6367.
(24) Ballmann, S.; Hieringer, W.; Secker, D.; Zheng, Q.; Gladysz, J. A.; Görling, A.; Weber, H. B. Molecular Wires in Single-Molecule Junctions: Charge Transport and Vibrational Excitations. *ChemPhysChem* **2010**, *11*, 2256−2260.
(25) Ballmann, S.; Hieringer, W.; Härtle, R.; Coto, P. B.; Bryce, M. R.; Görling, A.; Thoss, M.; Weber, H. B. The Role of Vibrations in Single-Molecule Charge Transport: A Case Study of Oligoynes With Pyridine Anchor Groups. *Phys. Status Solidi B* **2013**, *250*, 2452−2457.
(26) Cretu, O.; Botello-Mendez, A. R.; Janowska, I.; Pham-Huu, C.; Charlier, J.-C.; Banhart, F. Electrical Transport Measured in Atomic Carbon Chains. *Nano Lett.* **2013**, *13*, 3487−3493.
(27) Moreno-García, P.; Gulcur, M.; Manrique, D. Z.; Pope, T.; Hong, W.; Kaliginedi, V.; Huang, C.; Batsanov, A. S.; Bryce, M. R.; Lambert, C.; et al. Single-Molecule Conductance of Functionalized Oligoynes: Length Dependence and Junction Evolution. *J. Am. Chem. Soc.* **2013**, *135*, 12228−12240.
(28) Chalifoux, W. A.; McDonald, R.; Ferguson, M. J.; Tykwinski, R. R. *tert*-Butyl-End-Capped Polyynes: Crystallographic Evidence of Reduced Bond-Length Alternation. *Angew. Chem., Int. Ed.* **2009**, *48*, 7915−7919.
(29) Ford, M. S.; Anderson, M. L.; Barrow, M. P.; Woodruff, D. P.; Drewello, T.; Derrick, P. J.; Mackenzie, S. R. Reactions of Nitric Oxide on Rh_6^+ Clusters: Abundant Chemistry and Evidence of Structural Isomers. *Phys. Chem. Chem. Phys.* **2005**, *7*, 975−980.
(30) Anderson, M. L.; Ford, M. S.; Derrick, P. J.; Drewello, T.; Woodruff, D. P.; Mackenzie, S. R. Nitric Oxide Decomposition on Small Rhodium Clusters, $Rh_n^{\pm}$. *J. Phys. Chem. A* **2006**, *110*, 10992−11000.
(31) Kroto, H. W.; Heath, J. R.; O'Brien, S. C.; Curl, R. F.; Smalley, R. E. C_{60}: Buckminsterfullerene. *Nature* **1985**, *318*, 162−163.
(32) Clipston, N. L.; Brown, T.; Vasil'ev, Y. Y.; Barrow, M. P.; Herzschuh, R.; Reuther, U.; Hirsch, A.; Drewello, T. Laser-Induced Formation, Fragmentation, Coalescence, and Delayed Ionization of the $C_{59}N$ Heterofullerene. *J. Phys. Chem. A* **2000**, *104*, 9171−9179.
(33) Boorum, M. M.; Vasil'ev, Y. V.; Drewello, T.; Scott, L. T. Groundwork for a Rational Synthesis of C_{60}: Cyclodehydrogenation of a $C_{60}H_{30}$ Polyarene. *Science* **2001**, *294*, 828−831.
(34) Scott, L. T.; Boorum, M. M.; McMahon, B. J.; Hagen, S.; Mack, J.; Blank, J.; Wegner, H.; de Meijere, A. A Rational Chemical Synthesis of C_{60}. *Science* **2002**, *295*, 1500−1503.
(35) Kabdulov, M.; Jansen, M.; Amsharov, K. Y. Bottom-Up C_{60} Fullerene Construction From a Fluorinated $C_{60}H_{21}F_9$ Precursor by Laser-Induced Tandem Cyclization. *Chem.—Eur. J.* **2013**, *19*, 17262−17266.
(36) Tobe, Y.; Nakagawa, N.; Naemura, K.; Wakabayashi, T.; Shida, T.; Achiba, Y. [16.16.16](1,3,5)Cyclophanetetracosayne ($C_{60}H_6$): A Precursor to C_{60} Fullerene. *J. Am. Chem. Soc.* **1998**, *120*, 4544−4545.
(37) Rubin, Y.; Parker, T. C.; Pastor, S. J.; Jalisatgi, S.; Boulle, C.; Wilkins, C. L. Acetylenic Cyclophanes as Fullerene Precursors: Formation of $C_{60}H_6$ and C_{60} by Laser Desorption Mass Spectrometry of $C_{60}H_6(CO)_{12}$. *Angew. Chem., Int. Ed.* **1998**, *37*, 1226−1229.
(38) Tobe, Y.; Umeda, R.; Sonoda, M.; Wakabayashi, T. Size-Selective Formation of C_{78} Fullerene From a Three-Dimensional Polyyne Precursor. *Chem.—Eur. J.* **2005**, *11*, 1603−1609.
(39) McElvany, S. W.; Ross, M. M.; Goroff, N. S.; Diederich, F. Cyclocarbon Coalescence: Mechanisms for Tailor-Made Fullerene Formation. *Science* **1993**, *259*, 1594−1596.
(40) Ómarsson, B.; Bald, I.; Ingólfsson, O. Negative Ion Formation Mechanism and Velocity Distribution in Laser Desorption/Ionization of C_{60}. *Eur. Phys. J. D* **2012**, *66*, 1−7.
(41) Mamyrin, B. A. Laser Assisted Reflectron Time-Of-Flight Mass Spectrometry. *Int. J. Mass Spectrom. Ion Processes* **1994**, *131*, 1−19.
(42) Lou, X.; van Dongen, J. L. J.; Meijer, E. W. Generation of CsI Cluster Ions for Mass Calibration in Matrix-Assisted Laser Desorption/Ionization Mass Spectrometry. *J. Am. Soc. Mass. Spectrom.* **2010**, *21*, 1223−1226.
(43) Danell, R.; Danell, A.; Glish, G.; Vachet, R. The Use of Static Pressures of Heavy Gases Within a Quadrupole Ion Trap. *J. Am. Soc. Mass. Spectrom.* **2003**, *14*, 1099−1109.
(44) Yeretzian, C.; Hansen, K.; Diederich, F.; Whetten, R. L. Coalescence Reactions of Fullerenes. *Nature* **1992**, *359*, 44−47.
(45) Beck, R. D.; Stoermer, C.; Schulz, C.; Michel, R.; Weis, P.; Bräuchle, G.; Kappes, M. M. Enhanced Coalescence Upon Laser Desorption of Fullerene Oxides. *J. Chem. Phys.* **1994**, *101*, 3243−3249.
(46) Hillenkamp, F.; Peter-Katalinić, J. *MALDI MS: A Practical Guide to Instrumentation, Methods and Applications*; Wiley-VCH Verlag GmbH & Co. KGaA: Weinheim, Germany, 2007.
(47) Pasch, H.; Schrepp, W. *MALDI-TOF Mass Spectrometry of Synthetic Polymers*; Springer-Verlag GmbH: Heidelberg, Germany, 2003.
(48) Brown, T.; Clipston, N. L.; Simjee, N.; Luftmann, H.; Hungerbühler, H.; Drewello, T. Matrix-Assisted Laser Desorption/Ionization of Amphiphilic Fullerene Derivatives. *Int. J. Mass Spectrom.* **2001**, *210−211*, 249−263.
(49) Fati, D.; Leeman, V.; Vasil'ev, Y. V.; Drewello, T.; Leyh, B.; Hungerbühler, H. Alkali Cation Attachment to Derivatized Fullerenes Studied by Matrix-Assisted Laser Desorption/Ionization. *J. Am. Soc. Mass. Spectrom.* **2002**, *13*, 1448−1458.
(50) Kuvychko, I. V.; Streletskii, A. V.; Shustova, N. B.; Seppelt, K.; Drewello, T.; Popov, A. A.; Strauss, S. H.; Boltalina, O. V. Soluble Chlorofullerenes $C_{60}Cl_{24,46,48,10}$. Synthesis, Purification, Compositional Analysis, Stability, and Experimental/Theoretical Structure Elucidation, Including the X-ray Structure of C_1-$C_{60}Cl_{10}$. *J. Am. Chem. Soc.* **2010**, *132*, 6443−6462.
(51) Bottari, G.; Dammann, C.; Torres, T.; Drewello, T. Laser-Induced Azomethine Ylide Formation and Its Covalent Entrapment by Fulleropyrrolidine Derivatives During MALDI Analysis. *J. Am. Soc. Mass. Spectrom.* **2013**, *24*, 1413−1419.
(52) Streletskii, A. V.; Ioffe, I. N.; Kotsiris, S. G.; Barrow, M. P.; Drewello, T.; Strauss, S. H.; Boltalina, O. V. In-Plume Thermodynamics of the MALDI Generation of Fluorofullerene Anions. *J. Phys. Chem. A* **2005**, *109*, 714−719.
(53) Vasil'ev, Y. V.; Khvostenko, O. G.; Streletskii, A. V.; Boltalina, O. V.; Kotsiris, S. G.; Drewello, T. Electron Transfer Reactivity in Matrix-Assisted Laser Desorption/Ionization (MALDI): Ionization Energy, Electron Affinity and Performance of the DCTB Matrix Within the Thermochemical Framework. *J. Phys. Chem. A* **2006**, *110*, 5967−5972.
(54) Kellner, I. D.; Nye, L. C.; von Gernler, M. S.; Li, J.; Tzirakis, M. D.; Orfanopoulos, M.; Drewello, T. Ion Formation Pathways of Crown Ether-Fullerene Conjugates in the Gas Phase. *Phys. Chem. Chem. Phys.* **2014**, *16*, 18982−18992.
(55) Lungerich, D.; Hitzenberger, J. F.; Marcia, M.; Hampel, F.; Drewello, T.; Jux, N. Superbenzene−Porphyrin Conjugates. *Angew. Chem., Int. Ed.* **2014**, *53*, 12231−12235.
(56) Morin, J.-F. Oligoyne Derivatives as Reactive Precursors for the Preparation of Carbon Nanomaterials. *Synlett* **2013**, *24*, 2032−2044.

DOI: 10.1021/jp5112444
J. Phys. Chem. C 2015, 119, 2861−2870

(57) Yarimaga, O.; Jaworski, J.; Yoon, B.; Kim, J.-M. Polydiacetylenes: Supramolecular Smart Materials With a Structural Hierarchy for Sensing, Imaging and Display Applications. *Chem. Commun.* **2012**, *48*, 2469−2485.
(58) Bohlmann, F. Struktur und Reaktionsfähigkeit der Acetylen-Bindung. *Angew. Chem.* **1957**, *69*, 82−86.
(59) Wegner, G. Topochemical Reactions of Monomers With Conjugated Triple Bonds. *Z. Naturforsch., B: Chem. Sci.* **1969**, 824−832.

DOI: 10.1021/jp5112444
J. Phys. Chem. C 2015, 119, 2861−2870